Practical Paper

Practical Remote Sensing of Suspended Sediment Concentration

Jeffrey Liedtke, Arthur Roberts, and John Luternauer

Abstract

An airborne multispectral video (MSV) and small format photographic system was utilized to quantify suspended sediment concentrations (SSC) in a field experiment. Four video cameras with optical filtration for blue (415 to 485nm), green (515 to 585nm), red (615 to 685nm), and infrared (700 to 1150nm) were employed along with color and color infrared 35-mm film. The imagery was collected concurrently with surface sampling in the Fraser River sediment plume in the Strait of Georgia, British Columbia, Canada. Imagery was collected at 600 and 1200 metres above mean sea level (AMSL) to examine the influence of atmospheric factors on target reflectance. All imagery was digitized and regressed with SSC for prediction purposes.

Results demonstrated that narrow (10- to 16.8-mg/l) ranges of SSC can be estimated with multispectral video and small-format photographic imagery. Reflectance varied linearly for this relatively narrow range of mineral sediment concentrations. Simple linear regression equations are suitable for predicting SSC, with the red and green bands for all imagery being the strongest predictors. Sun angle corrections improved virtually all imagery, while dark-objection-subtraction techniques to compensate for atmospheric influences on imagery did not significantly improve results. After sun angle correction, green and red R^2 values for color film were 0.924 and 0.945, for color infrared film were 0.967 and 0.960, and 0.847 and 0.815 for MSV. These findings indicate that SSC can be adequately quantified using practical remote sensing systems and techniques.

Introduction

Marine studies are often limited by the inability to collect synoptic data. Extrapolation of surface sample results to unsampled areas are often tenuous and inaccurate because significant changes in conditions can occur over short distances and time periods, especially in estuarine and marine environments near deltas. Investigators examining water quality parameters and phenomena are also hampered by equipment, personnel, and cost constraints. Remote sensing data can overcome these difficulties by allowing analysis of complex circulation patterns and variable suspended sediment concentrations (SSC) in rapidly changing environments.

Multispectral remote sensing techniques have been used to identify or measure numerous water quality parameters (e.g., Khorram, 1979; Baban, 1993). Many studies have been successful in determining various aspects of sediment loads, including SSC, but have been limited by spatial, spectral and temporal resolution and atmospheric influences (Bowker *et al.*, 1975; Aranchuvachapun and LeBlond, 1981; Carpenter and Carpenter, 1983; Lathrop and Lillisand, 1989; Reddy, 1993). Landsat MSS and TM, SPOT, and NOAA AVHRR may not be particularly well suited for accurate analysis of water quality in esturine environments for a variety of reasons. Besides the relatively low spatial resolution of Landsat MSS and AVHRR, MSS and SPOT have wide, fixed spectral channels and lack a band in the blue-green spectral region, which is important for imaging water with low SSC and in bathymetric studies. Landsat TM can provide a viable option in some water quality studies (Lathrop, 1992) because the sensor features discrete non-overlapping channels and a channel in the blue-green spectral region, but with the unfortunate loss of Landsat-6, periodicity of coverage coupled with infrequent cloud-free days in the Pacific Northwest (Jardine *et al.*, 1993) and tropical regions still pose problems for studies in these areas.

Perhaps the most limiting factor in utilizing these satellite-borne sensors for water quality studies is that they were primarily designed for terrestrial applications (Tassan and Ribera d'Alcala, 1993). Terrestrial features reflect much more strongly than aquatic features, and the sensors are usually calibrated to accommodate the highly reflective features (i.e., low gain). Thus, the image density value range over water is usually very low and narrow. The relative atmospheric influence is much greater over water than land; Moore (1978) estimated that, over clear deep water, over 95 percent of the signal measured by Landsat MSS originated as atmospheric scattering caused by aerosol content alone. Additionally, electronic aberrations inherent in the sensors have a larger influence at these low spectral ranges than with the stronger return over land.

The flexibility offered by airborne sensors make them important tools for many kinds of remote sensing studies, and they can compliment and extend measurement made

J. Liedtke is with International Imaging Systems, 1500 Buckeye Drive, Milpitas, CA 95035.

A. Roberts is with the Department of Geography, Simon Fraser University, Burnaby, British Columbia V5A 1S6, Canada.

J. Luternauer is with the Geological Survey of Canada, 100 West Pender Street, 4th Floor, Vancouver, British Columbia V6B 1R8, Canada.

Photogrammetric Engineering & Remote Sensing,
Vol. 61, No. 2, February 1995, pp. 167–175.

0099-1112/54/6102-167$3.00/0

from traditional platforms (Harding *et al.*, 1992). Airborne sensors offer increased resolution and reduced atmospheric influences. In areas that experience frequent cloud cover, flights can be scheduled on arbitrary clear days, or missions can often be flown underneath cloud cover. Perhaps most importantly, flights can be planned to correspond with proper conditions to optimize information content of the target feature. Important mission parameters can be better controlled, such as time of day and year, project image scale, and near-real-time response to collect data associated with physical or environmental events.

Prior to 1968, when the first airborne multispectral scanners were being implemented, aerial photography was used to map water turbidity and depth (e.g., Moore, 1947; Jones, 1957). Aerial photography can provide satisfactory quantitative results with proper exposure and careful calibration techniques (Piech and Walker, 1971; Scherz and Van Domelsen, 1973; Villemonte *et al.*, 1974; Lillisand *et al.*, 1975). However, panchromatic film has a very wide spectral sensitivity, and the use of color-pack films result in the degradation of color separation images used in densitometric analysis. The red and green sensitive layers are partially exposed by blue light, i.e., color-pack films have overlapping spectral sensitivity between layers. For studies focusing on the radiometric characterization of features or phenomena, analyses using multilayered film result in reduced spectral resolution.

In light of some limitations of orbital multispectral scanners, the lack of spectral fidelity of color-pack films, and the high cost of airborne multispectral scanners, an alternative system for acquiring, processing, and analyzing remotely sensed water quality data for practical resource management is desirable. A low cost, spectrally suitable, and versatile remote sensing system needs to be developed for water quality analysis, along with compatible methodologies for information extraction from imagery collected with such a system. Both the sensor system and methods need to be developed so that a range of sediment conditions can be related on a spatial, spectral, and temporal basis. For example, an ideal system for acquiring and analyzing SSC data would be able to reliably determine variable SSCs in different geographical regions at different times. Important considerations that need to be addressed in formulating such an approach are

- knowledge of the energy-matter interactions in atmosphere and clear and turbid water;
- knowledge of the sensor system employed;
- appropriate control and compensation for extraneous influences of image data (e.g., atmospheric and system noise);
- proper data manipulation conforming to physical and statistical criteria;
- consistency of field sampling techniques and data handling; and
- applicability, in terms of analytical ability and cost.

There has been increased interest in multispectral video imaging systems which warrants closer examination of the attributes and capabilities of these low cost multispectral sensing systems. The rationale for using video are discussed in several straight-forward papers (Meisner and Lindstrom, 1985; Nixon *et al.*, 1985); the general advantages are that the imagery is already in an electronic format, is amenable to digital image processing techniques, and can be viewed, and even analyzed, in real time, allowing acquisition to occur under optimal conditions.

A substantial amount of analytical research has been conducted by researchers in the United States and Canada who have focused on range and crop applications (Escobar *et al.*, 1983; Mussakowski, 1984; Wu, 1989). Few studies have focused on quantifying water quality parameters. Mausel *et al.* (1989) examined the suitability of using an MSV system to determine turbidity in small lakes in west-central Indiana with promising results. Repic et al. (1991) used a multispectral video system to examine acidity and iron ore content in water collected in surface coal mines. An important benefit of utilizing video cameras is that they allow proper exposure adjustments to optimize image information content for the full range of sediment conditions. Additionally, sensor overflights can be coordinated with sun angles to minimize sun glint from the water surface, and can be closely timed with collection of surface samples using communication links between aircraft and surface sampling crews.

Study Area

The Fraser River drains almost a quarter of the province of British Columbia, Canada. The suspended sediment load varies with discharge, with most of the suspended material being silt and clay. Most suspended material is deposited south of the main stem at Roberts Bank, Boundary Bay and southward (Figure 1), greatly affecting the ecology in the Strait of Georgia and Puget Sound (Milliman, 1980). Saltwedge effects at the river's mouth and density differences between fresh and sea water cause the river water to flow over the dense salt water with little mixing. The Fraser River column is about 14 metres at the mouth of the main stem, and gradually thins to about a metre as it disperses across the Strait of Georgia in a south-southwest direction. Usually, a sharp contact exists between the turbid river water and the relatively clear marine water, delineated by a debris/foam line.

Along with the Tsawwassen Ferry Terminal, the Westshore Coal Terminal extends almost 2.5 kilometres into the

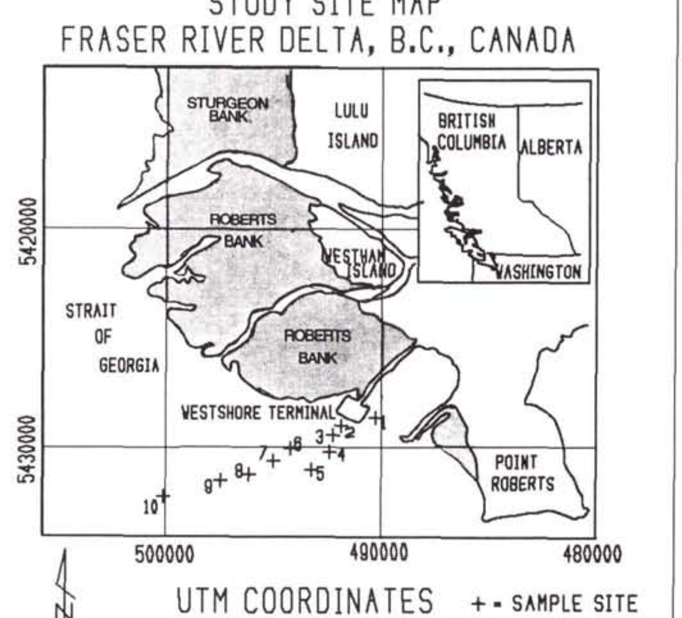

Figure 1. Study site map showing sampling site off the Westshore Terminals coal facility.

Strait of Georgia, protecting a man-made bay from heavy deposition of sediment (Figure 2). A wide range of sediment conditions exist; deep clear bay water separated from the areas having the highest SSCs by the Westshore Terminal, with SSC decreasing across the Strait of Georgia until clear sea water is encountered about 10 kilometres into the Strait of Georgia (Figure 1). Every overflight included imagery of coal wetted by water, which was used to help calibrate the imagery for atmospheric influences.

Methods

The remote sensing system used in this study included both electro-optical sensors and photographic systems. The MSV system was comprised of four video cameras with optical filters transmitting blue, green, red, and near infrared wavelengths. Two 35-mm cameras were used with Ektachrome and infrared Aerochrome film for comparison with the video imagery.

The video system, described by Roberts and Evans (1986), consisted of one Newvicon and three CCD low-light video cameras. Matched variable focal length (12.5 to 75mm) lenses were used with each camera, set at 75mm. A Newvicon and two CCDs were outfitted with blue (415 to 485nm), green (515 to 585nm), and red (615 to 685nm) band-pass interference filters, and a third CCD camera was used with a glass near-infrared sharpcut filter (88A: 700 to 1100+ nm). Acquired imagery was recorded on four individual 8-mm metal video cassette recorders. Proper camera exposures were set with the aid of a waveform monitor. Imagery from each camera was viewed by the operator during acquisition on a 6-inch black-and-white monitor through a switching system, while the pilot was able to verify proper coverage by viewing imagery from any one camera on a 4-inch monitor mounted in the aircraft's control panel.

Two 35-mm reconnaissance cameras were used to supplement the MSV imaging system. The Nikon F250s (with Nikkor 24-mm *f* 2.8 lenses) were used with

- Kodak Infrared Aerochrome 2443 and a Wratten 22 filter for haze penetration and blue light removal; and
- Kodak Ektachrome 5037 color film with a 85B filter for haze penetration and color balance.

Imagery from these cameras provided broad-band information covering the spectral gaps between the sensors of the MSV system, and allowed comparisons with the video imagery. The aircraft utilized was a Cessna 185-c (turbo, photo conversion) outfitted with photo hatches covered with optical glass. All cameras were boresighted for nadir viewing.

On 8 August 1986, a surface sampling transect was laid out from the Westshore Terminal extending southwest (240 degrees) into the Strait of Georgia for about 8 km. Winds were 0.5 m/sec from the north, and the sea state was moderately choppy with occasional whitecaps. Suspended sediment samples were collected at seven selected sites arranged along a sampling transect. The sampling sites were spaced apart by 500 to 1000m, and were identified by a 2.4-m floating target (Figures 1 and 2). A Canadian Coast Guard hovercraft and two small boats with outboard motors were used in surface sampling. The hovercraft's onboard navigation system was utilized to set up a straight transect in open waters and provided communication links between aircraft and sampling crews. The two small boats were launched from the Westshore Terminal and traveled to sites 1 and 2 nearest the coal terminal and collected samples every 5 minutes for 45 minutes, starting at 10:45AM. The hovercraft traveled between the remaining five sample sites collecting water samples. No target was laid at the clear water site because SSC was low and assumed to remain constant over the sampling period. The field survey sample size was 14 when data from the two overflights were combined. Sediment concentrations ranged from 10.6 mg/l to 16.8 mg/l; the "clear water" site had an SSC of 2.1 mg/l.

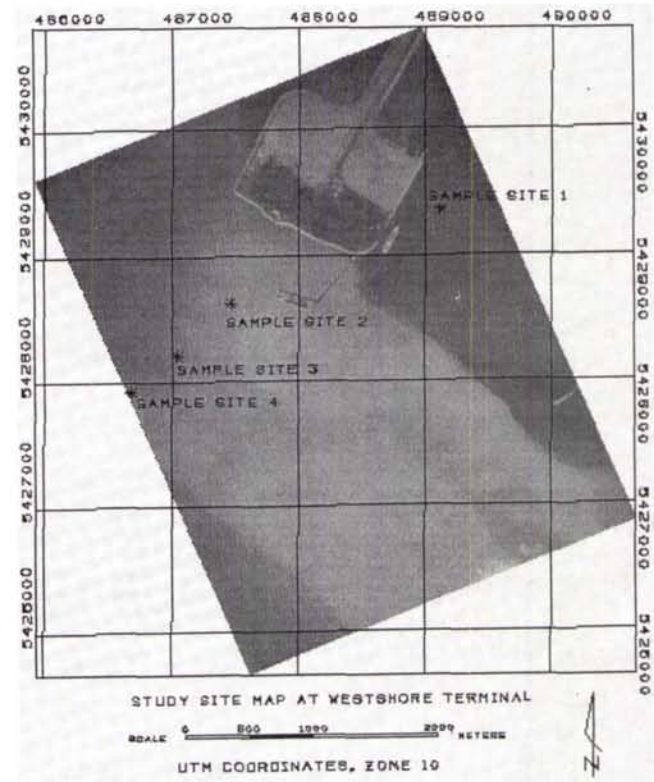

Figure 2. Sample site in the Fraser River sediment plume (sites 2-4) and clear water (site 1) adjacent to Westshore Terminals. Intensity image derived from Ektachrome color film.

The secchi disk disappearance depth was determined for each sampling site as an estimate of the remote sensing penetration depth. Two sampling baskets containing three and four weighted sampling bottles, respectively, were lowered to the secchi disappearance depth and raised at a constant rate to obtain seven integrated sediment samples at each of the seven sites. Each site was sampled at two different times during the mission. These samples were then analyzed to obtain the amount of sediment measured as mg/l.

Imagery was collected at two altitudes between 10:00 and 10:55. The first overflight was flown at 600 m above mean sea level (AMSL), and the second overflight was flown at an altitude of 1200 m AMSL. The time lag between sensor overflight and sample collection was usually only a few minutes, the longest being 20 minutes.

Image Analysis

Ektachrome color 5037 and Infrared Aerochrome 2443 films were analyzed with a transmission densitometer with red, green, and blue filters (Wratten 92, 93, and 94, respectively) that allowed measurement of film density for each of the three dye layers. Film density is inversely related to scene reflectivity, where a high optical count corresponds to low scene reflectivity. The color film was sensitive to blue, green, and red wavelengths, while the color infrared was sensitive to green, red, and reflected infrared wavelengths. Optical density counts were collected using a 1 mm aperture. The 1-mm aperture corresponded to a ground distance of 8 and 16 m for the imagery collected at 600 and 1200 m, respectively. Five densitometric readings were averaged for each sample point on all photographic images. The optical counts were then regressed with SSC and analyzed.

Video imagery lends itself to computer image processing due to its electronic format. Spectrally discrete video frames were digitized with a video digitizer, time base corrector with built-in master sync generator, and waveform monitor. The waveform monitor helped insure that the most information possible was captured without over- or under-saturation and loss of information. The different video intensities, represented by 0.01 to 1 volts (100 divisions) on the waveform monitor, were digitized into intensity levels between 0 and 255.

Only the pixels in the scene center were used for analysis, without registering the bands. This was done to avoid image registration difficulties posed by both the sensor system and the lack of easily identifiable surface reference points over water. Video frames selected for digitization were selected with the use of a stopwatch, VCR counter, and identification of identical water surface reflections. In order to average variation in the imagery due to sea-state or surface orientations, the reflectance data collected from the video images for the regression analysis were collected as a group of pixels adjacent to the sampling target. A region of interest (ROI) was delineated around the sampling site for each separate band. These ROIs were analogous to the densitometric spot reading from the film. The number of pixels within an ROI was about 300, representing a surface area of about 8 square metres for the 600-m imagery, from which the mean and standard deviation of the region were used in the subsequent regression analysis. Because the ROI was located in the center of the frame, camera and lens distortions were reduced, thus avoiding complex camera and radiometric calibrations procedures.

Clear water has low reflectance and can be used as both a dark object for subtraction from imagery for atmospheric compensation and as a standard with which to compare turbid water bodies. Subtraction of the minimum reflectance value of clear water from turbid water (in each band) results in the subtraction of approximately the atmospheric reflectance from the water surface and the volume reflectance of clear water. Thus, the residual reflectance is attributed to SSC (Scarpace *et al.*, 1979; Scherz and Van Domelsen, 1975; Sydor, 1980).

Statistical Analysis Methods

Many researchers have used regression techniques to estimate a variety of water quality parameters with varying degrees of success (Johnson, 1975; Whitlock and Kuo, 1979; Whitlock *et al.*, 1982). The theoretical justification for using this particular method is well described by Whitlock (1977). The remote sensing signal responses to various concentrations of different constituents suspended in water (in terms of optical physics) can be summarized in a straight-forward manner by multiple regression equations. Regression models for predicting SSC were developed between surface truth measurements (dependant variable) and reflectance values (independent variables) represented by densitometric optical counts (film) or grey density numbers (electronic sensors).

Measures of Adequacy

It was not known how many channels, or in what combination, would be required to make a reliable prediction of SSC. Several statistical parameters were used as indicators of precision of the regression equation. These parameters were

- Coefficient of determination (R^2), which describes the variation of SSC explained by the combined linear influence of reflectance for the different channels;
- Standard error of the estimate, SE;
- the F-values, at the 0.95 confidence level, as an overall test for goodness of fit for the regression equation; and
- Total squared error, called the C_p statistic. C_p measures the sum of the squared biases plus the sum of the squared errors for the dependant variables at all n data points. Given a multiple regression equation with P estimated coefficients, a low value of C_p coupled with a C_p/P ratio of less than 1.0 is indicative of a good fit with negligible bias.

Thus, the criteria used to select the optimum regression equation to predict SSC were (Whitlock, 1977)

- The correlation coefficient (r) should be as high as possible,
- the $R^2 \geq 0.70$,
- the standard error of the estimate (SE) should approach 0,
- the $F/F0.05 \geq 4.0$,
- the total squared error (C_p) should be low, and
- the C_p/P ratio ≤ 1.0.

Results

The analytical capability of the airborne multispectral video and photographic system was evaluated in terms of sensitivity and precision in predicting SSC. The first step was to determine which bands or film layers responded best to various sediment concentrations, then to evaluate the predictive capabilities of these bands using linear and log-linear multiple regression techniques. Data with sun angle compensation, dark-object-subtraction, and band ratios were regressed with SSC. Results illustrated a clear relationship between SSC and scene reflectance, with reflectance increasing with increasing SSC. Regression values and other measures of adequacy show that single-term equations were suitable for the statistical prediction of SSC. Results of linear regressions are tabulated in Tables 1, 2, and 3. Film optical density numbers (DN) were inversely related to SSC (i.e., low DN is high SSC) (Figures 3, 4, 5, and 6), while MSV DNs increase linearly with SSC (Figures 7 and 8).

Results from the study tended to be strong for both the multispectral video and aerial photography for the two individual overflights at 600 and 1200 m AMSL, with the strongest results from the imagery collected at 600 m, due to increased atmospheric influence and greater sun angle at 1200 m. The overflight at 600 m occurred at 10:45 PST, while imagery collected at 1200 m occurred at 11:30, resulting in a difference of 3 degrees in sun angle and in higher scene reflectance. R^2 values generally decreased further when data from both overflights were combined, producing a sample size of 14. When combined, regression lines of the two altitudes were offset, indicating that sun angle differences between overflights affected the amount of atmospheric scattering. Atmospheric scattering was greatest in the blue channel, while the infrared channel was affected the least, as expected. Results from combining film data from both overflights were generally improved by multiplying DN values by

TABLE 1. STATISTICS FOR KODAK EKTACHROME 5037 (COLOR)

	Band	r	R^2	SE	F
1	R	0.996	0.991	0.437	671.502
	G	0.993	0.986	0.551	419.608
	B	0.998	0.996	0.305	138.544
2	R	0.970	0.941	1.126	95.906
	G	0.973	0.946	1.078	105.126
	B	0.961	0.923	1.288	71.823
3	R	0.958	0.917	1.237	154.670
	G	0.944	0.891	1.420	114.006
	B	0.802	0.644	2.563	25.314
4	R	0.972	0.945	1.006	241.359
	G	0.961	0.924	1.182	170.850
	B	0.849	0.720	2.271	36.082

R = the Red channel
G = the Green channel
B = the Blue channel
1 = data collected at 600 m AMSL
2 = data collected at 1200 m AMSL
3 = data collected at 600 and 1200 m combined
4 = data collected at 600 and 1200 m adjusted for sun angle differences

TABLE 2. STATISTICS FOR KODAK INFRARED AEROCHROME 2443

	Band	r	R^2	SE	F
1	IR	0.875	0.765	2.221	19.562
	R	0.992	0.985	0.564	390.448
	G	0.991	0.982	0.608	334.930
2	IR	0.789	0.623	2.815	9.911
	R	0.968	0.937	1.153	88.873
	G	0.975	0.952	1.009	117.848
3	IR	0.892	0.688	2.371	30.881
	R	0.979	0.958	0.868	320.616
	G	0.981	0.963	0.813	367.205
4	IR	0.803	0.644	2.531	25.362
	R	0.980	0.960	0.849	335.711
	G	0.983	0.967	0.775	405.61

IR = the InfraRed channel
R = the Red channel
G = the Green channel
1 = data collected at 600 m AMSL
2 = data collected at 1200 m AMSL
3 = data collected at 600 and 1200 m combined
4 = data collected at 600 and 1200 m adjusted for sun angle differences

TABLE 3. STATISTICS FOR MULTISPECTRAL VIDEO IMAGERY (MSV)

	Band	r	R^2	SE	F
1	IR	0.961	0.924	1.283	73.119
	R	0.914	0.835	1.890	30.432
	G	0.967	0.936	1.182	87.108
	B	0.844	0.712	2.498	14.858
2	IR	0.871	0.759	2.276	18.930
	R	0.938	0.880	1.608	43.919
	G	0.923	0.851	1.789	34.333
	B	0.884	0.781	2.169	21.444
3	IR	0.903	0.815	1.854	61.477
	R	0.914	0.835	1.748	70.893
	G	0.902	0.813	1.859	61.065
	B	0.851	0.725	2.257	36.913
4	IR	0.916	0.839	1.729	72.786
	R	0.903	0.815	1.853	61.505
	G	0.920	0.847	1.683	77.547
	B	0.842	0.709	2.321	34.145

IR = the InfraRed channel (700-1150 nm)
R = the Red channel (615-685 nm)
G = the Green channel (515-585 nm)
B = the Blue channel (415-485 nm)
1 = data collected at 600 m AMSL
2 = data collected at 1200 m AMSL
3 = data collected at 600 and 1200 m combined
4 = data collected at 600 and 1200 m adjusted for sun angle differences.

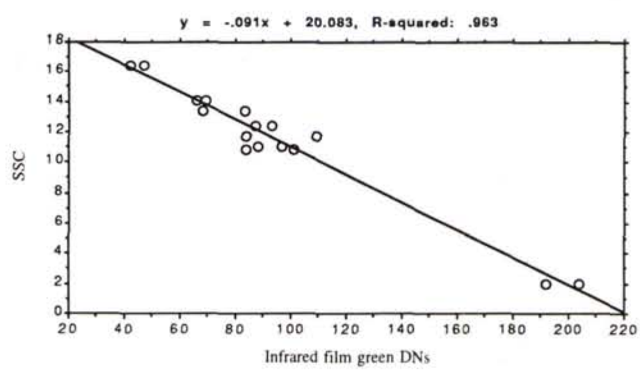

Figure 3. Relationship between SSC and infrared film green DNs.

the cosine of the sun angle, while MSV results were generally improved by multiplying DNs by the sine of the sun angle. Dark-object-subtraction techniques did not significantly improve either the film or MSV results. Results from film and MSV are addressed in turn.

Film Analysis

The optical density counts for each dye layer of the color and infrared films, representing film density, were regressed with SSC. All of the film layers of both film types were good predictors of SSC for overflights at both altitudes, with stronger results from the data collected at 600 m. When data from both flights were combined to increase the sample size to 14, regression coefficients and number of variables meeting the statistical criteria decreased. Red and green film layers gave strong results for both color and infrared film, with IR-film red and green R^2 values higher than values from the color film (Tables 1 and 2 and Figures 3 and 4). Statistical values for the infrared film remained high, indicating that it was relatively unaffected by atmospheric and sun angle differences between the two flights. Probable reasons for this are due to filtration (Wratten 22) blocking wavelengths shorter than 560 nm and reduced atmospheric scattering in near infrared.

The blue-sensitive layer from the color film had high regression coefficients for the individual flightlines (Table 1). The blue R^2 decreased from 0.996 to 0.923 for overflights at 600 and 1200 m, respectively, to 0.644 when data from both overflights were combined. The green and red sensitive layers were affected somewhat less by atmospheric and sun an-

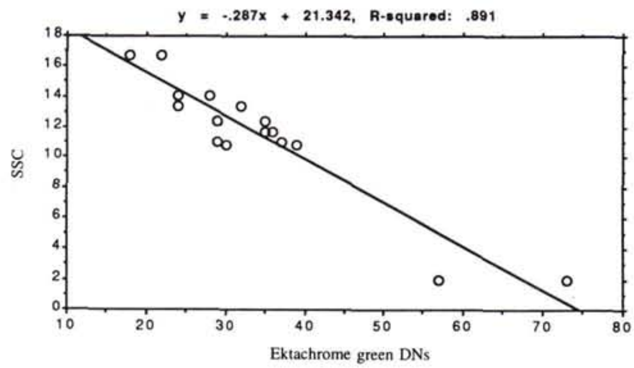

Figure 4. Relationship between SSC and Ektachrome film green DNs.

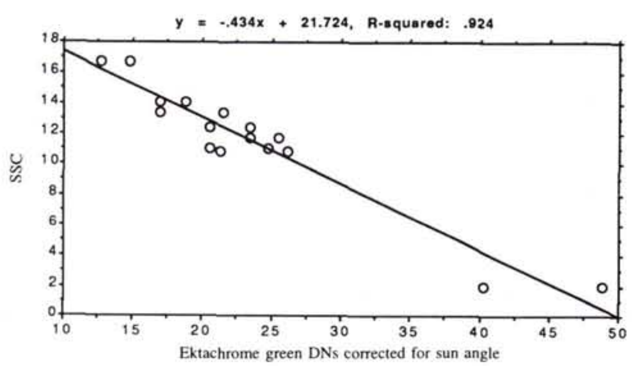

Figure 5. Relationship between SSC and Ektachrome green DNs corrected for sun angle.

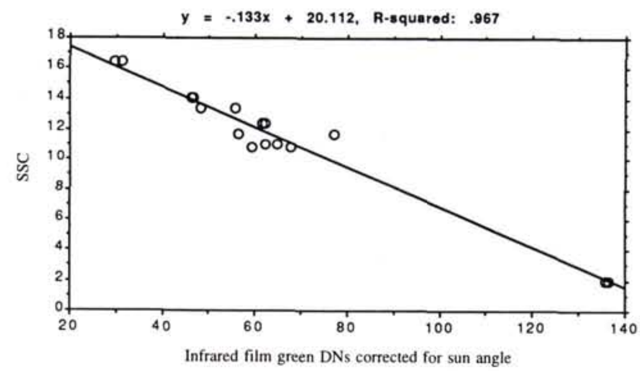

Figure 6. Relationship between SSC and infrared film green DNs corrected for sun angle.

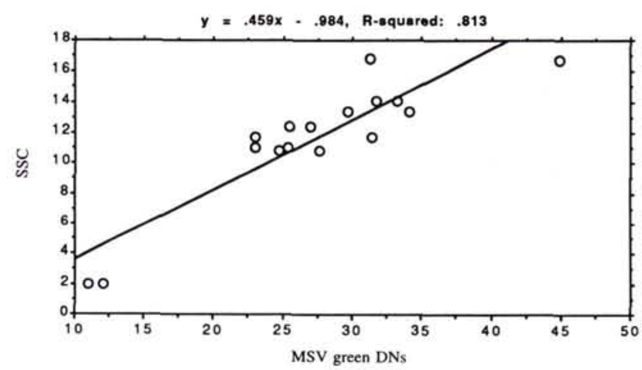

Figure 7. Relationship between SSC and MSV green DNs.

gle influences, with R^2 values of 0.891 and 0.917, respectively, when both overflights were combined.

In order to compensate for increased sun angle between the two flights, film density counts were multiplied by the cosine of the sun angle (Liedtke, 1988). Results using IR film improved slightly, while the R^2 values of color film red and green layers improved significantly from 0.917 and 0.891 to 0.945 and 0.924, respectively (Figures 4 and 5). Because shorter wavelengths are scattered more than longer wavelengths, atmospheric scattering had a presumably reduced effect on the infrared film and a stronger effect on the color film. Sun angle correction also brought the blue regression lines from both overflights into closer registration, but blue was still affected by increased atmospheric scattering between the flights. Sun angle correction improved virtually all film results with the two overflights combined.

The strongest predictor of SSC for all film was the green band of the IR film corrected for sun angle differences between overflights (R^2 0.967, Figure 6), the regression equation being

$$y = -0.133x + 20.112$$

while the normalized red band provided the best results (R^2 .945) for the color film: i.e.,

$$y = -0.334x + 22.497$$

where y is the predicted sediment concentration and x is the image DN, or reflectance value.

Analysis of Multispectral Video

The four video bands analyzed were blue, green, red, and infrared. The DNs were proportional to reflectance, so that a large DN represents high reflectivity (Figure 7). Tables of the regression analyses and the summary statistics are compiled in Table 3. R^2 values derived from the MSV imagery were not as high as those for film, but R^2 values were above 0.70 for all bands for both overflights. The green and red channels yielded the best results, similar to film. The MSV IR band performed better than the IR film layer, and suggests that the IR band is useful for predicting variable SSC along with red and green.

The response of the blue band was similar to the film in that it was sensitive to changing SSC at low altitudes, but was affected by atmospheric scattering and sun angle differences between the two altitudes. While the R^2 values of the blue band remained greater than 0.7 with flights combined, blue had the lowest R^2 value of all bands, similar to the blue film layer. When data acquired from 600 and 1200 m were combined, R^2 values of the red and green bands decreased but remained strong, with R^2 values of 0.835 and 0.813, re-

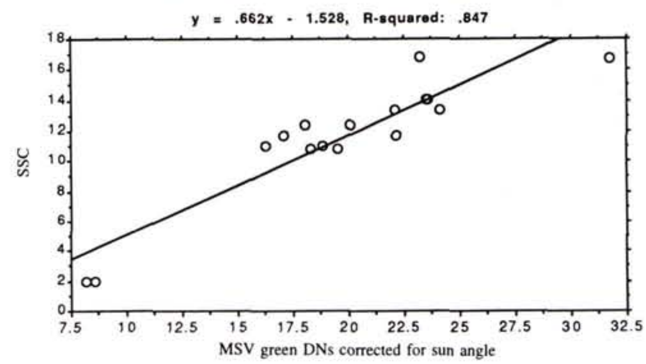

Figure 8. Relationship between SSC and MSV green DNs corrected for sun angle.

spectively. IR results actually improved with the two flights combined. Similar to film, this indicates that IR is less affected by atmospheric scattering and sun angle influences.

In the video digitization process, there was evidence that the time base corrector (TBC) was making some exposure adjustments. The "black pedestal" on the TBC was set too high, so that dark objects such as the Westshore Terminals coal and very clear water were saturated to black (DN value 0). Unfortunately, this adjustment of very low DNs rendered their use in dark-object-subtraction (DOS) procedures for compensation of additive atmospheric influences inappropriate. It is expected that proper implementation of DOS procedures will yield stronger results, similar to the film results.

Multiplying the DNs by the sine of the sun angle did not improve the results for the red and blue bands, indicating that the imagery was affected by other extraneous factors besides sun angle, e.g., probable sensor noise. Values for the IR and green bands were improved by the sun angle correction, with the R^2 for green improving from 0.813 to 0.847 (Figure 8). The regression equation for the MSV green band corrected for sun angle differences was

$$y = 0.662x - 1.528$$

where y is the predicted sediment concentration and x is the green band DN, or reflectance value.

Summary

These findings demonstrated that suspended sediment concentrations could be quantified using practical remote sensing systems and techniques. The results from the individual flightlines were good, with red and green R^2 values for all imagery greater than 0.81, low standard error, and minimum bias. R^2 values were highest for individual overflights because atmospheric influences were calibrated into the regression equations. Combining data from both flight lines reduced the statistical strength of the derived regression equations to predict SSC due to increased atmospheric and sun angle influences and noise. In order for these remote sensing techniques to have more universal utility, the data must be corrected for sun angle and atmospheric influences. Data from the two flight lines were combined to test procedures such as dark object subtraction and sun angle correction.

Because the range in sediment concentration was relatively narrow in the field study (10.6 to 16.8 mg/l), the spectral shift of peak reflectivity from green to red wavelengths found with higher SSC conditions did not occur. Therefore, both bands experienced a similar increase in overall reflectance with increased SSC, and the relative behavior of the increased reflectance was similar. Consequently, neither band ratios nor logarithmic relationships improved the predictive equations.

The green band was the best predictor of SSC at both altitudes for all imagery, similar to the findings of Whitlock *et al.* (1978). In another airborne study, Poinke and Blanchard (1975) found that green wavelengths (530 to 580 nm) were the most responsive to narrow sediment ranges, while orange (588 to 643 nm) together with red (650 to 680 nm) was the best combination to predict broad ranges of SSC (13 to 232 mg/l). The performance of the red band was also consistently good at both altitudes for all imagery, similar to Johnson and Bahn (1977). Green and red R^2 values for the color infrared film gave the best results, 0.967 and 0.960, respectively, after sun angle correction. Green and red R^2 values were also strong for color film (0.945 and 0.924). While results of film analysis were generally stronger than those using MSV imagery, the performance of the MSV green and red bands was good (0.847 and 0.815). The MSV IR channel was a better predictor of SSC than was the film IR. The MSV system needs to be tested in a variety of environmental and physical conditions to assess its overall utility and reliability for quantification of SSC and additional water quality parameters. Subsequent studies indicate that the MSV system is sensitive to a wide range of sediment concentrations (31 to 380 mg/l; Liedtke, 1988).

While this study is practical in nature, it is stressed that data collection and analysis procedures were based on physical and statistical criteria conforming to remote sensing scientific methodologies, and the project design was guided by these criteria. The remote sensing techniques used to quantify SSC were regression analysis, sun angle correction, and dark-object-subtraction to normalize the data. The good results coupled with the many advantages of video systems and imagery make the utility of MSV a favorable option to using highly technical and expensive remote sensing systems. Small format photography and multispectral video systems may provide local, county, and regional agencies a practical and viable option for gathering and analyzing important information for many water quality studies. Possible applications include determining sediment transport paths, wetlands habitat assessments and monitoring (Roberts and Liedtke, 1986), dredging and shipping, and environmental monitoring.

Acknowledgments

The Geological Survey of Canada made this research possible by providing equipment, logistical, and financial support. We acknowledge and thank the airborne and surface sampling crews for their superb efforts and commitment.

References

Aranuvachapun, S., and P.H. LeBlond, 1981. Turbidity of Coastal Water Determined from Landsat, *Remote Sensing of Environment*, 84:113–132.

Baban, S.M.J., 1993. Detecting Water Quality Parameters in the Norfolk Broads, U.K., Using Landsat Imagery, *International Journal of Remote Sensing*, 14(7):1247–1267.

Bowker, D.E., W.G. Witte, F. Fleischer, T.A. Gosnik, W.G. Hanna, and J.C. Ludwick, 1975. An Investigation of the Waters in the Lower Chesapeake Bay Area, *Proceedings, 10th International Symposium on Remote Sensing of Environment*, 1:411–420.

Carpenter, D.J., and S.M. Carpenter, 1983. Modeling Inland Water Quality Using Landsat Data, *Remote Sensing of Environment*, 1: 483–489.

Escobar, D.E., R.L. Bowen, H.W. Gausman, and G. Cooper, 1983. Use of Near-Infrared Video Recording System for the Detection of Freeze-damaged Citrus Leaves, *Journal Rio Grande Valley Horticultural Society*, Vol. 36.

Everitt, J.H., A.J. Richardson, D.E. Escobar, and R. Villarreal, 1989. Mapping Native Plant Communities with Color-Infrared Video Imagery, *Twelfth Biennial Workshop on Color Aerial Photography and Videography in the Plant Sciences and Related Fields*, pp. 30–38.

Harding, L.W., Jr., E.C. Itsweire, and W.E. Esaias, 1992. Determination of Phytoplankton Chlorophyll Concentrations in the Chesapeake Bay with Aircraft Remote Sensing, *Remote Sensing of Environment*, 40:79–100.

Jardine, I.D., K.A. Thomson, M.G. Foreman, and P.H. LeBlond. 1993. Remote Sensing of Coastal Sea-Surface Features off Northern British Columbia, *Remote Sensing of Environment*, 45:73–84.

Johnson, R.W., 1975. Quantitative Suspended Sediment Mapping Using Aircraft Remotely Sensed Multispectral Data, *NASA Earth Resources Survey Symposium*, 1-C:2097–2098.

Johnson, R.W., and G.S. Bahn, 1977. *Quantitative Analysis of Aircraft Multispectral Scanner Data and Mapping of Water Quality Parameters in the James River in Virginia*, NASA Technical Paper 1021, 31 p.

Jones, B.C., 1957. Photogrammetric Surveys for National Charts, *Photogrammetic Engineering*, 23:291–298.

Khorram, S., 1979. Remote Sensing Analysis of Water Quality in the San Francisco Bay Delta, *Proceedings, 13th International Symposium on Remote Sensing of Environment*, 3:1591–1598.

Lathrop, R.G., Jr., 1992. Landsat Thematic Mapper Monitoring of Turbid Inland Water Quality, *Photogrammetric Engineering & Remote Sensing*, 58(4):465–470.

Lathrop, R.G., and T.M. Lillisand, 1989. Monitoring Water Quality and River Plume Transport in Green Bay, Michigan with SPOT-1 Imagery, *Photogrammetric Engineering & Remote Sensing*, 55(3):349–354.

Liedtke, Jeff, 1988. *Discrimination of Suspended Sediment Concentrations Using Multispectral Remote Sensing Techniques*, Master of Science Publication, Department of Geography, Simon Fraser University, British Columbia, Canada, pp. 72–93.

Lillisand, T.M., F.L. Scarpace, and J.L. Clapp, 1975. Water Quality in Mixing Zones, *Photogrammetric Engineering & Remote Sensing*, (41):285–xxx.

Mausel, P.W., M.A. Karaska, and C.Y. Mao, 1989. Insights into Water Turbidity Through Computer Analysis of Multispectral Video Analysis, *Twelfth Biennial Workshop on Color Aerial Photography and Videography in the Plant Sciences and Related Fields*, pp. 216–226.

Meisner, D.E., and O.M. Lindstrom, 1985. Design and Operation of a Color Infrared Aerial Video System, *Photogrammetric Engineering & Remote Sensing*, 51(5):555–560.

Milliman, J., 1980. Sedimentation in the Fraser River and its Estuary, Southwest British Columbia, Canada, *Esturine and Coastal Marine Science*, 10:609–633.

Moore, G.K. 1978. Satellite Surveillance of Physical Water-Quality Characteristics, *Proceedings, 12th International Symposium on Remote Sensing of Environment*, 1:445–462.

Moore, J., 1947. The Determination of Depths of Extinction Coefficients of Shallow Water by Air Photography Using Color Filters, *Royal Society Philosophical Transcripts*, 240(816), London.

Mussakowski, R.S., 1984. The Application of video Remote Sensing to Resource Surveys and Environmental Monitoring, *9th Canadian Symposium on Remote Sensing, Proceedings*, pp. 203–208.

Nixon, P.R., D.E. Escobar, and R.M. Menges, 1985. A Multiband Video System for Quick Assessment of Vegetal Condition and Discrimination of Plant Species, *Remote Sensing of Environment*, 17:203–208.

Piech, K.R., and J.E. Walker, 1971. Aerial Color Analysis of Water Quality, *Journal of the Surveying and Mapping Division*, Proceedings, American Society of Civil Engineers, pp. 185–197.

Pionke, H.B., and B.J. Blanchard, 1975. The Remote Sensing of Suspended Sediment Concentrations of Small Impoundments, *Water, Air and Soil Pollution*, 4:19–32.

Reddy, M.A., 1993. Remote Sensing for Mapping of Suspended Sediments in Krishna Bay Esturay, Andhra Pradesh, India, *International Journal of Remote Sensing*, 14(11):2215–2221.

Repic, R., J.K. Lee, P.W. Mausel, D.E. Escobar, and J. Everitt, 1991. An Analysis of Selected Water Parameters in Surface Coal Mines Using Multispectral Videography, *Photogrammetric Engineering & Remote Sensing*, 57(12):1589–1596.

Roberts, A., and D. Evans, 1986. Multispectral Video System for Airborne Remote Sensing, *Proceedings, 10th Canadian Symposium on Remote Sensing*, Edmonton, Alberta Canada.

Roberts, A., and J. Liedtke, 1986. Airborne Definition of Suspended Surface Sediment and Intertidal Environments in the Fraser River Plume, British Columbia, *Current Research, Part A, Geological Survey of Canada, Paper 86-1A*, pp. 571–582.

Scarpace, F.L., K.W. Holmquist, and L.T. Fisher, 1979. Landsat Analysis of Water Quality, *Photogrammetric Engineering & Remote Sensing*, 45:623–633.

Scherz, J.P., and J.F. Van Domelsen, 1973. Lake Superior Water Quality Near Duluth from Analysis of Aerial Photos and ERTS Imagery, *Remote Sensing and Water Resources Management, American Water Resources Association, Proceedings*, No. 17.

Sydor, M., 1980. Remote Sensing of Particulate Concentrations in Water, *Applied Optics*, 19(16):2794–2800.

Tassan, S., and M. Ribera d'Alcala, 1993. Water Quality Monitoring by Thematic Mapper in Coastal Environments. A Performance Analysis of Local Biooptical Algorithms and Atmospheric Correction Procedures, *Remote Sensing of Environment*, 45:177–191.

Villemonte, J.J., D. Wu, and T. Lillisand, 1974. Remote Sensing in the Mixing Zone, *Remote Sensing and Water Resources Management, American Water Resources Association, Proceedings*, No. 17.

Whitlock, C.H., 1977. *Fundamental Analysis of the Linear Multiple Regression Technique for Quantification of Water Quality Parameters From Remote Sensing Data*, Thesis, NASA Technical Memorandum X-74600, NASA, Johnson Center.

Whitlock, C.H., G. Witte, and J.W. Usry, 1978. Penetration Depth at Green Wavelengths in Turbid Waters, *Photogrammetric Engineering & Remote Sensing*, 44(11):1405–1410.

Whitlock, C.H., and C.Y. Kuo, 1979. A Regression Technique For Evaluation and Quantification of Water Quality Parameters From Remote Sensing Data, *Proceedings, 13th International Symposium on Remote Sensing of Environment*, 3:1351–1365.

Wu, Shih-Tseng, 1989. Utility of a Digital Video and Image Analysis System For Forest and Coastal Wetlands Mapping, *Twelfth Biennial Workshop on Color Aerial Photography and Videography in the Plant Sciences and Related Fields*, pp. 164–170.

(Received 6 June 1993; accepted 20 October 1993; revised 13 December 1993)

Jeff Liedtke

Jeff Liedtke is the Marketing Manager for International Imaging Systems in California, where he has been employed for seven years. Mr. Liedtke is responsible for assisting clients in developing solutions for their applications, transfer of technology by supporting educational and research institutions, and identifying and helping to implement new

innovative capabilities through I²S Engineering and Marketing Departments to satisfy client's applications.
Mr. Liedtke received his MSc. Degree in Geography at Simon Fraser University, B.C., Canada, in 1987, where he assisted in the development and implementation of an airborne multispectral video system for quantifying suspended sediment in marine environments. He received Bachelor Degrees in Geography and Environmental Studies from University of California, Santa Barbara, in 1982. Between 1981 and 1983 he worked with the Los Padres National Forest Land Management Planning Team to generate both working and published maps for all land use prescription scenarios. GIS coverages were generated and manipulated as necessary to model management scenarios, resulting in a detailed Forest Plan submitted to the U. S. Forest Service Headquarters, Washington, D.C.

Arthur Roberts
Arthur Roberts is currently Associate Professor, Department of Geography, Simon Fraser University. He received his B.A., University of Toronto, 1971; M.A., Waterloo, Geography, 1977; and Ph.D., York University, Geography, 1982. Research Associate, Department of New World Archaeology, Royal Ontario Museum. Executive, S.F.U. Institute for Quaternary Research. Chair, S.F.U. Spatial Information Systems Committee, Editorial Board, International Journal of Remote Sensing. Member, S.F.U. Centre for Systems Science. Publications: 1 book, 28 refereed publications; 35 other publications; 47 conference papers. Graduate spervision: senior supervision 18 students; committee member 12 students; examiner 8 students. Organizations: American Association for the Advancement of Science; American Society of Photogrammetry; Canadian Aeronautical and Space Institute; Canadian Owners and Pilots Association; Canadian Remote Sensing Society; Royal Canadian Geographical Society; S.F.U. Centre for Systems Science; S.F.U. Institute for Quaternary Research.

John L. Luternauer
John L. Luternauer, Ph.D., P.Geo., received his doctorate in Marine Geology from the University of British Columbia in 1972 after completing research on the Late Quaternary evolution of the central continental shelf of western Canada. He joined the Geological Survey of Canada in 1974 after publishing his post doctoral research on the sedimentary processes and budget of the Freaser River delta front. During his term with the GSC he has investigated geohazards to the coastal and offshore developments, sediment/groundfish associations, continental shelf placer deposits and the role of sea level history on migration of early humans in western Canada.